Facile solid-phase synthesis of the diammoniate of diborane and its thermal decomposition behavior

ARTICLE *in* PHYSICAL CHEMISTRY CHEMICAL PHYSICS · MARCH 2011

Impact Factor: 4.49 · DOI: 10.1039/c1cp00018g · Source: PubMed

8 AUTHORS, INCLUDING:

X.D. Kang
Chinese Academy of Sciences
61 PUBLICATIONS **1,456** CITATIONS

PCCP

View Online
Dynamic Article Links

Cite this: *Phys. Chem. Chem. Phys.*, 2011, **13**, 7508–7513

www.rsc.org/pccp

PAPER

Facile solid-phase synthesis of the diammoniate of diborane and its thermal decomposition behavior†

Zhanzhao Fang,[a] Junhong Luo,[a] Xiangdong Kang,[a] Haijie Xia,[a] Sisheng Wang,[b] Wen Wen,[b] Xingtai Zhou[b] and Ping Wang*[a]

Received 4th January 2011, Accepted 22nd February 2011
DOI: 10.1039/c1cp00018g

The recent mechanistic finding of the hydrogen release pathways from ammonia borane (AB) has sparked new interest in the chemistry and properties of the diammoniate of diborane (DADB), an ionic isomer of AB. We herein report a facile one-step solid-phase synthesis route of DADB using inexpensive starting materials. Our study found that mechanically milling a 1 : 1 $NaBH_4/NH_4F$ powder mixture causes the formation of crystalline DADB *via* a NH_4BH_4 intermediate. The produced DADB can be readily separated from the sodium fluoride (NaF) by-product by a purification procedure using liquid ammonia at −78 °C. The thermal decomposition behavior of DADB was studied using synchronous thermal analyses, particularly in comparison with AB. It was found that the decomposition steps and products of DADB are similar to those of AB. But meanwhile, DADB exhibits a series of advantages over AB that merit its potential hydrogen storage application, such as lower dehydrogenation temperature, free of foaming and lack of an induction period in the thermal decomposition process. Our study further found that the volatile non-hydrogen products from DADB can be effectively suppressed by milling with MgH_2.

1. Introduction

The development of hydrogen-powered vehicles requires advanced materials that can store and deliver large amounts of hydrogen at moderate temperatures with fast kinetics.[1,2] Recently, ammonia borane (NH_3BH_3, AB) has received considerable attention as a promising hydrogen storage medium.[3–10] AB possesses extremely high hydrogen density (19.6 wt%) and particularly it is a unique molecular crystal containing both hydridic and protonic hydrogen.[11,12] The H_2 release from AB is thermodynamically favored, but greatly kinetically impeded at ambient temperatures.[3,4] Adding to this kinetic problem are the competitive side-reactions that yield volatile by-products.[3,6–9] In the past years, several strategies have been developed to address these problems, such as using metal catalysts to promote the dehydrocoupling or hydrolysis reactions,[13–19] confinement into nanoporous scaffolds,[3,8] addition of chemical promoters,[4,6,20–22] and chemical modification of AB through substitution of the amine hydrogen with metal cations.[23–26] These technological advances have resulted in significant improvements on the dehydrogenation properties of AB. In particular, several AB-based materials, which show potential in satisfying many of the principal criteria for an on-board hydrogen source, have been successfully synthesized.[20–24] This progress has further inspired the exploration of other related B-N-H compounds for potential hydrogen storage applications.

The diammoniate of diborane ($[(NH_3)_2BH_2]^+[BH_4]^-$, DADB), an ionic isomer of AB, is a stable crystalline solid at ambient conditions. DADB was first synthesized in 1923,[27] but until quite recently, this hydrogen-rich material never received serious consideration as a hydrogen carrier. This situation was changed by Autrey *et al.*, whose *in situ* solid-state NMR study demonstrated that the formation of DADB through isomerization of AB is a critical nucleation event leading to H_2 release from thermolysis of AB.[5] This finding raises interest in evaluating the H_2 release property of DADB. But the study of DADB is severely restricted by the material availability. The earlier syntheses of DADB involve the direct reaction of diborane (B_2H_6) and ammonia (NH_3) at cryogenic temperatures.[27–31] The usage of highly toxic and flammable reactants, the rigorous manipulation requirements and the slowness of the procedure make the early synthesis routes ill adapted to large-scale production. Quite recently, Autrey *et al.* reported the successful synthesis of DADB by reacting NH_4F and $NaBH_4$ in liquid NH_3, followed by decomposition of the resultant ammonium borohydride (NH_4BH_4) at room temperature.[32] This method permits for the first time the facile synthesis of authentic DADB. Herein, we report an alternative and even more efficient mechanochemical synthetic route of DADB.

[a] *Shenyang National Laboratory for Materials Science, Institute of Metal Research, Chinese Academy of Sciences, Shenyang 110016, China. E-mail: pingwang@imr.ac.cn*
[b] *Shanghai Synchrotron Radiation Facility, Shanghai Institute of Applied Physics, Chinese Academy of Sciences, Shanghai 201204, China*
† Electronic supplementary information (ESI) available. See DOI: 10.1039/c1cp00018g

Our study found that mechanically milling a 1 : 1 $NaBH_4$/NH_4F powder mixture followed by extraction with liquid NH_3 produces DADB in high yield. Thus-prepared DADB was further examined by synchronous thermal analyses to evaluate its potential for hydrogen storage applications.

2. Experimental

All the powdery chemicals, $NaBH_4$ (98%), NH_4F (98%), AB (97%) and MgH_2 (98%), were purchased from Sigma-Aldrich Corp. and used as received. The mechanochemical synthesis of DADB from the 1 : 1 $NaBH_4$/NH_4F powder mixture was carried out under argon (99.999%) atmosphere in a Fritsch 7 planetary mill at 200 rpm using a stainless steel vial together with eight steel balls. The ball-to-powder ratio was around 150 : 1. The post-milled sample with a typical amount of ~500 mg was loaded into a three-neck round-bottom flask containing ~50 ml liquid NH_3. The extraction and filtration were carried out at −78 °C. DADB polycrystalline powder was finally obtained by vacuum distilling NH_3 from the filtrate. Except for the extraction process, all sample handling was performed in an Ar-filled glovebox, which was equipped with a circulative purification system to maintain the H_2O and O_2 levels typically below 0.1 ppm.

The thermal decomposition behavior of DADB and related samples was examined by synchronous thermal analyses (thermogravimetry/differential scanning calorimetry/mass spectroscopy; TG/DSC/MS, Netzsch 449C Jupiter/QMS 403C). In the thermal analyses, the samples were heated to 400 °C at a ramping rate of 5 °C min^{-1} under a flowing Ar (99.999%) atmosphere.

The post-milled $NaBH_4$/NH_4F and DADB samples were characterized by powder X-ray diffraction (XRD, Rigaku D/MAX-2500, Cu-Kα radiation), Fourier transform infrared spectroscopy (FTIR, Bruker TENSOR 27, DLaTGS detector, 4 cm^{-1} resolution) and solid-state ^{11}B MAS NMR (Varian Infinityplus-400 spectrometer, operated at 9.4 T with a ^{11}B resonance frequency of 128.3 MHz). All the sample preparations were carried out in the argon-filled glovebox, and special measures were taken to minimize H_2O/O_2 contamination during the sample transfer process. FTIR spectra of the samples were collected using the KBr-pellets method and normalized using OPUS 6.5 software. The details of solid-state ^{11}B MAS NMR measurements can be found in ref. 24. The purified sample was also examined using a high-resolution synchrotron X-ray powder diffractometer at the beamline BL14B1 of the Shanghai Synchrotron Radiation Facility (SSRF) at a wavelength of 1.2398 Å.

3. Results and discussion

3.1 Mechanochemical synthesis of DADB

DADB can be readily produced by mechanically milling the $NaBH_4$/NH_4F powder mixture in a 1 : 1 molar ratio. This was confirmed by the combined XRD, FTIR and NMR results. As shown in Fig. 1(a), the diffraction peaks of the starting materials ($NaBH_4$ and NH_4F) completely disappeared after ball milling for 3 h, and the newly formed phases can be indexed to DADB (JCPDS17-0269)[30] and the by-product

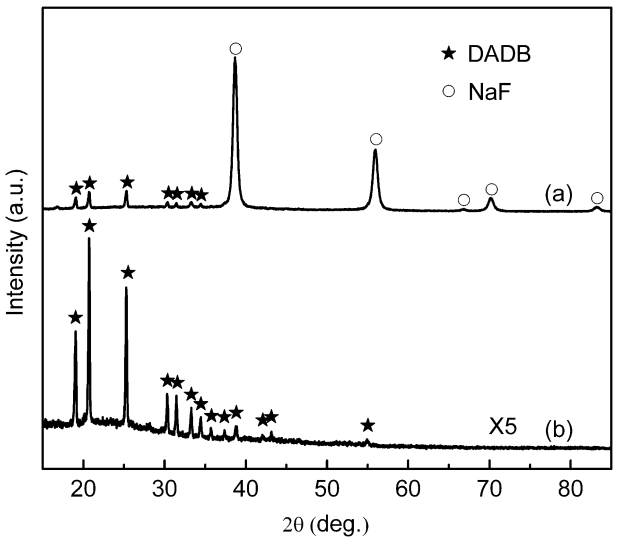

Fig. 1 XRD patterns of (a) the post-milled $NaBH_4$/NH_4F sample and (b) that after the purification procedure.

NaF. The FTIR pattern of the post-milled sample, as shown in Fig. 2(a), agrees well with the literature result of DADB that was prepared by Carpenter and Ault using the matrix isolation technique.[33] Additionally, the $^{11}B\{^1H\}$ MAS NMR spectrum presented in Fig. 3 clearly showed the characteristic resonances at −35 to −38 and −14.1 ppm that correspond to the BH_4^- and BH_2 of DADB, respectively.[32] Furthermore, the observed resonance splitting in the BH_4^- region is in excellent accordance with the two crystallographically distinct BH_4^- sites in DADB that was recently demonstrated by Autrey *et al.*[32] These structural results strongly suggest that the solid-phase reaction following eqn (1) occurs in the milling process, resulting in the formation of DADB. This was further supported by the observed gas evolution in the milling process, which amounts to about 1 mole per mole of $NaBH_4$ (or NH_4F) after 3 h milling.

$$2NaBH_4 + 2NH_4F \rightarrow DADB + 2NaF + 2H_2 \quad (1)$$

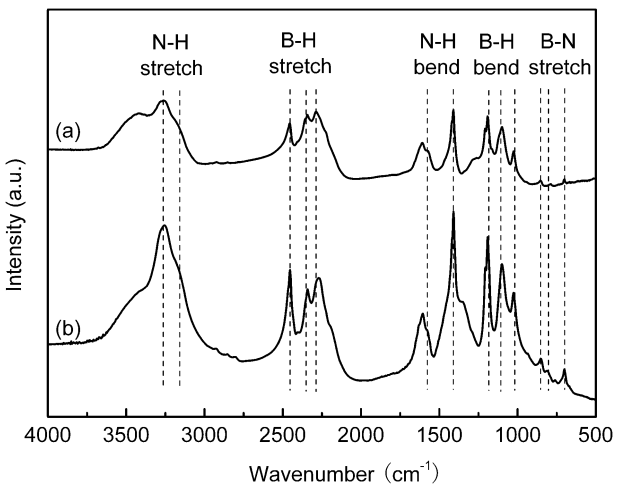

Fig. 2 FTIR patterns of (a) the post-milled $NaBH_4$/NH_4F sample and (b) that after the purification procedure.

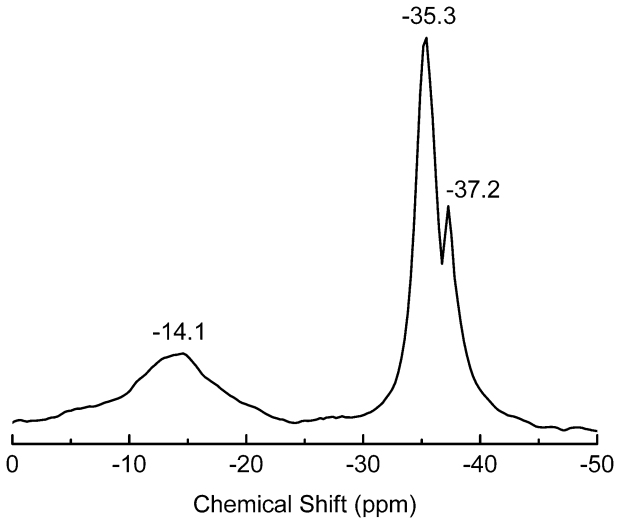

Fig. 3 $^{11}B\{^{1}H\}$ MAS NMR spectrum of the post-milled $NaBH_4/NH_4F$ sample.

The mechanochemical synthesis of DADB using $NaBH_4$ and NH_4F as starting materials involves the concomitant formation of NaF. Fortunately, the NaF by-product can be readily removed in an extraction procedure using liquid NH_3 as solvent. As seen in Fig. 1(b), the purified sample only showed the diffraction peaks of DADB. The parallel FTIR analysis of the purified sample (Fig. 2(b)) gave an identical spectrum to that of the post-milled $NaBH_4/NH_4F$ sample.

These results indicated that the applied purification procedure introduces no contamination to DADB. The milling-driven solid-phase reaction, in conjunction with the extraction process using liquid NH_3, therefore provides a simple, efficient and easily practised synthesis route of DADB. Furthermore, this convenient procedure is combined with the usage of cheap materials, which makes it easily adaptable to large-scale production. In our bench-scale preparation, yields of DADB of over 95% were consistently obtained. Thus-prepared DADB was found to be structurally stable at ambient temperature for at least 30 days (Fig. S1 and S2, ESI†).

In an effort to determine the crystal structure of DADB, we examined the purified sample using a high-resolution synchrotron radiation X-ray diffractometer. The XRD pattern of DADB (Fig. S3, ESI†) can be indexed to a body-centered tetragonal structure in space group $I4/mcm$ with parameters $a = b = 10.74$ Å and $c = 9.25$ Å. Our result agrees well with the latest finding of Autrey *et al.*,[32] thus further supporting the validity of the structure solution.

3.2 Mechanistic study of the formation of DADB

A series of designed experiments were conducted to gain insight into the formation mechanism of DADB. First, we examined the phase evolution of the 1 : 1 $NaBH_4/NH_4F$ powder mixture in the milling process. As seen in Fig. 4(a), the XRD pattern of the sample after milling for 20 min is dominated by the strong diffraction peaks of the newly formed NH_4BH_4 (in a rock salt structure)[34,35] and NaF phases. But the solid-phase reaction is clearly incomplete at this stage, since the diffraction peaks of $NaBH_4$ were still detectable. Here, the invisibility of the diffraction peaks of NH_4F is an indication of its amorphous nature. After extending the milling time to 40 min (Fig. 4(b)), the diffraction peaks of $NaBH_4$ completely disappeared and the weak peaks of DADB became detectable, which was accompanied with a significant intensity decrease of NH_4BH_4. When the milling time was further extended to 120 min (Fig. 4(d)), the XRD pattern only showed the presence of crystalline DADB and NaF. These results clearly indicate that the solid-phase reaction between $NaBH_4$ and NH_4F proceeds through an intermediate NH_4BH_4 to the final product of DADB. Therefore, eqn (1) should be rewritten as eqn (2) to more precisely describe the reaction scheme. This finding suggests that the synthesis route of DADB from the 1 : 1 $NaBH_4/NH_4F$ mixture in a mechanochemical process is actually similar to that reported by Autrey *et al.*[32] A major difference between the two synthesis procedures is that our procedure combines the formation and decomposition of NH_4BH_4 in the mechanochemical process, which appears more convenient and efficient in the practical operation.

$$2NaBH_4 + 2NH_4F \rightarrow 2NH_4BH_4 + 2NaF \rightarrow DADB + 2NaF + 2H_2 \quad (2)$$

The latest studies by Autrey *et al.* demonstrated that the decomposition of NH_4BH_4 to DADB involves an intermediate and transient formation of AB.[32,34] Our study found that this mechanism may also be applicable for the mechanochemical synthesis of DADB. As seen from the comparison of Fig. 4 and 5, the addition of AB to the $NaBH_4/NH_4F$ mixture markedly promoted the formation of DADB. For example, it takes around 120 min for the $NaBH_4/NH_4F$ mixture to completely transform into DADB and NaF (Fig. 4(d)). In contrast, the $NaBH_4/NH_4F$/AB sample completed the solid-phase reaction within 20 min under identical milling conditions (Fig. 5(b)). This was further confirmed by the parallel FTIR analysis, which shows the complete disappearance of the characteristic B–N stretching modes of AB after milling for 20 min (Fig. S4, ESI†). Here, the high reactivity of AB towards NH_4BH_4, in conjunction with the solvent-free preparation condition, may account for the selective formation of DADB rather than AB.[29]

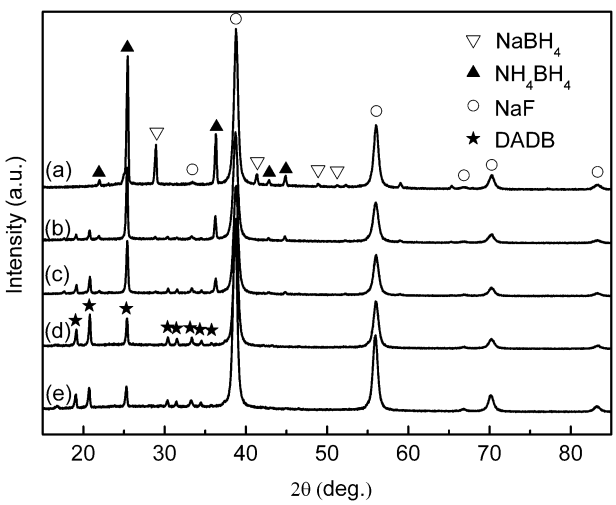

Fig. 4 XRD patterns of the $NaBH_4/NH_4F$ samples that were milled for (a) 20 min; (b) 40 min; (c) 60 min; (d) 120 min; and (e) 180 min.

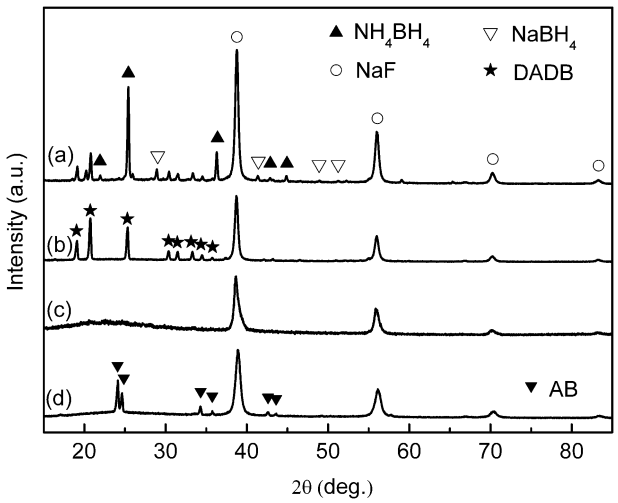

Fig. 5 XRD patterns of the $NaBH_4/NH_4F/x$AB samples after milling for 20 min: (a) $x = 0.5$; (b) $x = 1$; (c) $x = 2$. The sample examined in (d) was prepared by milling the $NaBH_4/NH_4F$ mixture for 2 h, followed by addition of AB and milling for another 20 min.

Interestingly, when we further increased the added amount of AB to a 1 : 1 : 2 molar ratio, the post-milled sample showed no diffraction peaks of DADB and AB (Fig. 5(c)). But in the parallel FTIR analysis, the characteristic B–N stretching modes of both DADB and AB were clearly identified (Fig. S4, ESI†). These results suggested that the amorphization of DADB and AB occurs in the milling process, most probably as a consequence of the solid-phase interaction. To gain further insight into this amorphization phenomenon, we first prepared DADB by ball milling the 1 : 1 $NaBH_4/NH_4F$ mixture for 2 h, and then added AB for another 20 min milling. The XRD result (Fig. 5(d)) showed the presence of crystalline AB and amorphous DADB in the post-milled sample. This result is important as it showed clearly that the presence of excessive AB causes amorphization of DADB, whereas DADB exerts no influence on the crystalline structure of AB. Accordingly, the observed amorphization of excess AB in the post-milled $NaBH_4 + NH_4F + 2$AB sample might be associated with the NH_4BH_4 intermediate. This was proven true especially after ruling out the possible roles of $NaBH_4$, NH_4F, DADB and NaF for the amorphization of AB (Fig. S5, ESI† and Fig. 5(d)). Obviously, the amorphization of AB is an indication of its strong interaction with the NH_4BH_4 intermediate, which should be essentially correlated with the high reactivity of amorphous AB towards NH_4BH_4. This provides us a valuable hint for the mechanistic understanding of the interactions between AB and NH_4BH_4. Presumably, NH_4BH_4 first induces the amorphization of AB, and then reacts with amorphous AB to produce DADB. In this regard, detailed experimental and theoretical studies are still required to further the mechanistic understanding towards the solid-phase interactions between AB and NH_4BH_4.

3.3 Thermal decomposition behavior of DADB

The purified DADB was further studied and compared with AB in terms of thermal decomposition behavior. As seen in Fig. 6, both materials show two distinct exothermic decomposition steps at temperatures below 200 °C. According to the *ex situ* XRD (Fig. S6, ESI†) and FTIR analyses (Fig. S7 and S8, ESI†), the decomposition products of DADB are also quite similar to those of AB, *i.e.*, the amorphous polyaminoborane $[(NH_2BH_2)_n]$- and polyiminoborane $[(NHBH)_n]$-like species formed after the first and second decomposition step, respectively. Except for these similarities, DADB also exhibits several notable differences from its isomer AB in terms of thermal decomposition behavior. First, the temperature threshold for decomposition is about 10 °C lower than that of AB. Second, the mass loss (25.5 wt%) from DADB upon heating up to 300 °C is much lower than that (53.9 wt%) from AB, indicative of the significantly reduced evolution of volatile by-products. Third, DADB undergoes solid-phase decomposition without melting. Fourth, unlike AB, the thermal decomposition of DADB is free of foaming. And fifth, DADB exhibits no appreciable induction period even at moderate temperature, while AB suffers from a long induction period (> 10 h) prior to H_2 release (Fig. S9, ESI†). Apparently, these features merit the potential hydrogen storage application of DADB.

Evolution of volatile non-hydrogen products is one of the major problems of DADB that restricts its potential hydrogen storage application. As seen in Fig. 7, DADB releases considerable amounts of diborane (B_2H_6) and borazine ($B_3N_3H_6$) at the second decomposition step and ammonia (NH_3) throughout the heating process up to 400 °C, which should qualitatively account for the larger mass loss (~ 30 wt%) than that expected for releasing 2 equiv. H_2 (~ 13 wt%). Differing from our results, Autrey *et al.* claimed that their DADB samples released no significant quantity of NH_3 at temperatures up to 200 °C.[32] One possible reason for this difference may be the variation of the synthesis procedure.

Our preliminary study found that mechanically milling with MgH_2 can effectively suppress the evolution of volatile by-products from DADB. As seen from the MS results in Fig. 7, the post-milled DADB/MgH_2 sample releases no B_2H_6, $B_3N_3H_6$ and NH_3 within the detection limit of our MS apparatus. Besides the notable effect of suppressing gas impurities, the addition of MgH_2 also causes significant changes in the H_2 release behavior of DADB. The two dehydrogenation steps of DADB at temperatures below 200 °C were

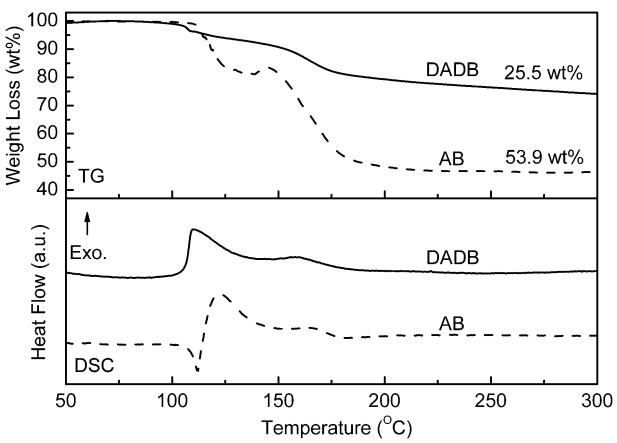

Fig. 6 Comparison of TG/DSC profiles of DADB (solid lines) and AB (dash lines). The heating rate was 5 °C min^{-1}.

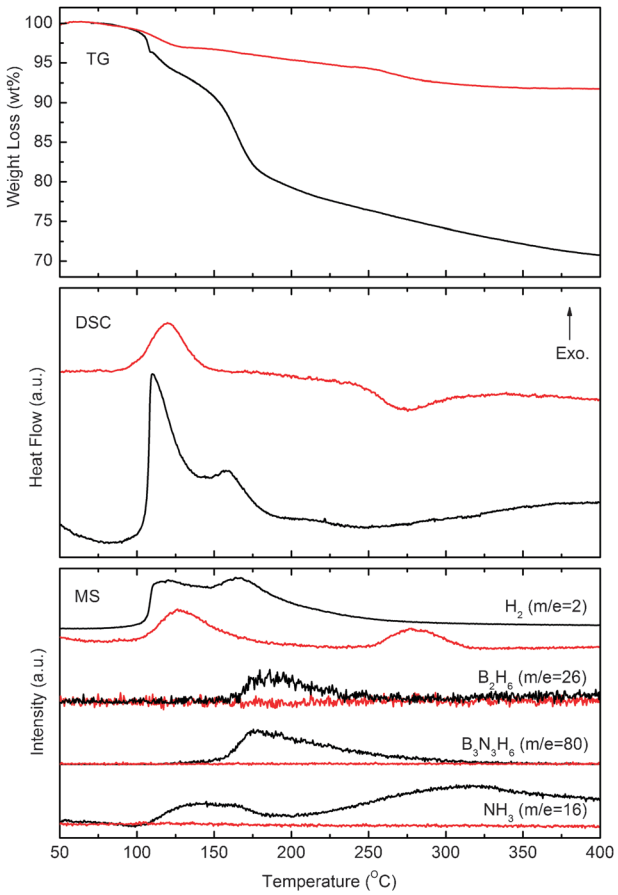

Fig. 7 Comparison of TG/DSC/MS profiles of DADB (black lines) and a post-milled DADB/MgH_2 sample (red lines). The heating rate was 5 °C min^{-1}.

found to merge into one step at 125 °C, and a new endothermic dehydrogenation step appears at around 275 °C for the DADB/MgH_2 sample. Fundamentally, these dramatic property changes should be correlated with the strong solid-phase interaction between DADB and MgH_2. A combination of XRD and FTIR analyses (Fig. S10 and S11, ESI†) found that the crystalline structure of DADB was completely disrupted after milling with MgH_2 for 30 min, and meanwhile the chemical bonding state of DADB was also significantly altered. In addition, it was observed that the diffraction intensity of MgH_2 became significantly weakened after heating the sample to 300 °C, suggesting that a considerable amount of MgH_2 actively participated in the dehydrogenation reactions. Currently, our study of the interaction mechanism between DADB and MgH_2 is still ongoing.

4. Conclusions

Mechanically milling a 1 : 1 $NaBH_4/NH_4F$ powder mixture, followed by extraction with liquid NH_3, provides a facile and high-yield solid-phase synthesis route of DADB. An important mechanistic step in this synthesis route is the formation of the NH_4BH_4 intermediate, which then decomposes to produce DADB. Pristine DADB shows similarities to its isomer AB on the decomposition steps and products. Meanwhile, DADB does exhibit a series of advantages over AB that merit its potential hydrogen storage application, such as lower dehydrogenation temperature, free of foaming in the thermal decomposition process and lack of induction period. A preliminary study has found that the evolution of volatile non-hydrogen products can be effectively suppressed by mechanically milling DADB with MgH_2. The results of this study should be helpful for the development of DADB as a promising hydrogen storage material.

Acknowledgements

Financial support from the National Natural Science Foundation of China (#50801059), the National Basic Research Program of China (973 Program, #2010CB631305 and 2010CB934500), the National High-Tech R&D Program of China (863 Program, #2009AA05Z109), the Main Direction Program of Knowledge Innovation of CAS, the Science and Technology Commission of Shanghai Municipality (#1052nm07800), and the CAS Special Grant for Postgraduate Research, Innovation and Practice is gratefully acknowledged. We also acknowledge beamline BL14B1 (SSRF) for providing the beam time.

References

1 L. Schlapbach and A. Züttel, *Nature*, 2001, **414**, 353.
2 U. Eberle, M. Felderhoff and F. Schüth, *Angew. Chem., Int. Ed.*, 2009, **48**, 6608.
3 A. Gutowska, L. Li, Y. Shin, C. M. Wang, X. S. Li, J. C. Linehan, R. S. Smith, B. D. Kay, B. Schmid, W. Shaw, M. Gutowski and T. Autrey, *Angew. Chem., Int. Ed.*, 2005, **44**, 3578.
4 D. J. Heldebrant, A. Karkamkar, N. J. Hess, M. Bowden, S. Rassat, F. Zheng, K. Rappe and T. Autrey, *Chem. Mater.*, 2008, **20**, 5332.
5 A. C. Stowe, W. J. Shaw, J. C. Linehan, B. Schmid and T. Autrey, *Phys. Chem. Chem. Phys.*, 2007, **9**, 1831.
6 D. Neiner, A. Karkamkar, J. C. Linehan, B. Arey, T. Autrey and S. M. Kauzlarich, *J. Phys. Chem. C*, 2009, **113**, 1098.
7 D. Neiner, A. Luedtke, A. Karkamkar, W. Shaw, J. Wang, N. D. Browning, T. Autrey and S. M. Kauzlarich, *J. Phys. Chem. C*, 2010, **114**, 13935.
8 Z. Y. Li, G. S. Zhu, G. Q. Lu, S. L. Qiu and X. D. Yao, *J. Am. Chem. Soc.*, 2010, **132**, 1490.
9 T. He, Z. T. Xiong, G. T. Wu, H. L. Chu, C. Z. Wu, T. Zhang and P. Chen, *Chem. Mater.*, 2009, **21**, 2315.
10 F. Y. Cheng, H. Ma, Y. M. Li and J. Chen, *Inorg. Chem.*, 2007, **46**, 788.
11 C. W. Hamilton, R. T. Baker, A. Staubitz and I. Manners, *Chem. Soc. Rev.*, 2009, **38**, 279.
12 F. H. Stephens, V. Pons and R. T. Baker, *Dalton Trans.*, 2007, 2613.
13 C. A. Jaska, K. Temple, A. J. Lough and I. Manners, *J. Am. Chem. Soc.*, 2003, **125**, 9424.
14 M. C. Denney, V. Pons, T. J. Hebden, D. M. Heinekey and K. I. Goldberg, *J. Am. Chem. Soc.*, 2006, **128**, 12048.
15 N. Blaquiere, S. Diallo-Garcia, S. I. Gorelsky, D. A. Black and K. Fagnou, *J. Am. Chem. Soc.*, 2008, **130**, 14034.
16 R. J. Keaton, J. M. Blacquiere and R. T. Baker, *J. Am. Chem. Soc.*, 2007, **129**, 1844.
17 X. Z. Yang and M. B. Hall, *J. Am. Chem. Soc.*, 2008, **130**, 1798.
18 J. M. Yan, X. B. Zhang, S. Han, H. Shioyama and Q. Xu, *Angew. Chem., Int. Ed.*, 2008, **47**, 2287.
19 T. J. Clark, G. R. Whittell and I. Manners, *Inorg. Chem.*, 2007, **46**, 7522.
20 X. D. Kang, L. P. Ma, Z. Z. Fang, L. L. Gao, J. H. Luo, S. C. Wang and P. Wang, *Phys. Chem. Chem. Phys.*, 2009, **11**, 2507.

21 J. H. Luo, X. D. Kang and P. Wang, *J. Phys. Chem. C*, 2010, **114**, 10606.
22 J. H. Luo, X. D. Kang and P. Wang, *ChemPhysChem*, 2010, **11**, 2152.
23 Z. T. Xiong, C. K. Yong, G. T. Wu, P. Chen, W. Shaw, A. Karkamkar, T. Autrey, M. O. Jones, S. R. Johnson, P. P. Edwards and W. I. F. David, *Nat. Mater.*, 2008, **7**, 138.
24 X. D. Kang, Z. Z. Fang, L. Y. Kong, H. M. Cheng, X. D. Yao, G. Q. Lu and P. Wang, *Adv. Mater.*, 2008, **20**, 2756.
25 H. Wu, W. Zhou and T. Yildirim, *J. Am. Chem. Soc.*, 2008, **130**, 14834.
26 H. V. K. Diyabalanage, R. P. Shrestha, T. A. Semelsberger, B. L. Scott, M. E. Bowden, B. L. Davis and A. K. Burrell, *Angew. Chem., Int. Ed.*, 2007, **46**, 8995.
27 A. Stock and E. Kusz, *Ber. Dtsch. Chem. Ges.*, 1923, **56B**, 789.
28 H. I. Schlesinger and A. B. Burg, *J. Am. Chem. Soc.*, 1938, **60**, 290.
29 R. W. Parry and S. G. Shore, *J. Am. Chem. Soc.*, 1958, **80**, 8; *J. Am. Chem. Soc.*, 1958, **80**, 15.
30 S. G. Shore and K. W. Böddeker, *Inorg. Chem.*, 1964, **3**, 914.
31 R. W. Parry, *J. Chem. Educ.*, 1997, **74**, 512.
32 M. Bowden, D. J. Heldebrant, A. Karkamkar, T. Proffen, G. K. Schenter and T. Autrey, *Chem. Commun.*, 2010, **46**, 8564.
33 J. D. Carpenter and B. S. Ault, *J. Phys. Chem.*, 1991, **95**, 3502.
34 A. Karkamkar, S. M. Kathmann, G. K. Schenter, D. J. Heldebrant, N. Hess, M. Gutowski and T. Autrey, *Chem. Mater.*, 2009, **21**, 4356.
35 R. Flacau, C. I. Ratcliffe, S. Desgreniers, Y. S. Yao, D. D. Klug, P. Pallister, I. L. Moudrakovski and J. A. Ripmeester, *Chem. Commun.*, 2010, **46**, 9164.